DALTON
FULL PAPER

Synthesis, structure and spectroelectrochemical properties of a dinuclear ruthenium complex exhibiting a strong electronic interaction across a 1,2,4,5-tetrazine bridging ligand

Biprajit Sarkar,[a] Rebecca H. Laye,[b] Biplab Mondal,[a] Soma Chakraborty,[a] Rowena L. Paul,[b] John C. Jeffery,[b] Vedavati G. Puranik,[c] Michael D. Ward *[b] and Goutam Kumar Lahiri *[a]

[a] *Department of Chemistry, Indian Institute of Technology, Mumbai-400076, India*
[b] *School of Chemistry, University of Bristol, Cantock's Close, UK Bristol BS8 ITS*
[c] *Physical Chemistry Division, National Chemical Laboratory, Pune, Maharastra-411008, India*

Received 13th September 2001, Accepted 11th February 2002
First published as an Advance Article on the web 3rd April 2002

The reaction of $[Ru(bpy)_2(EtOH)_2]^{2+}$ (bpy = 2,2′-bipyridine) with the potentially bridging ligand 3,6-bis(3,5-dimethylpyrazol-1-yl)-1,4-dihydro-1,2,4,5-tetrazine) (H_2L) results in formation of the diruthenium complex $[(bpy)_2Ru^{II}(L)Ru^{II}(bpy)_2]^{4+}$ ($[\mathbf{1}]^{4+}$) in which the dihydrotetrazine unit of H_2L has undergone oxidative dehydrogenation to give an aromatic tetrazine unit connecting the two metal centres [L = 3,6-bis(3,5-dimethylpyrazol-1-yl)-1,2,4,5-tetrazine]. The crystal structures of H_2L and $[\mathbf{1}(ClO_4)_4]\cdot 2H_2O$ have been determined. In MeCN solution, complex $[\mathbf{1}]^{4+}$ undergoes two successive one-electron oxidation processes at 1.25 and 1.70 V *versus* SCE, corresponding to successive Ru(II)/Ru(III) couples, affording a stable mixed-valence Ru(II)/Ru(III) state ($K_c = 4 \times 10^7$) at intermediate potentials. Four successive ligand-based reduction processes at −0.13, −0.99, −1.58 and −1.94 V *versus* SCE are also observed, of which the first two are associated with the bridging tetrazine unit and the other two are reductions of the coordinated bipyridine molecules. A UV/VIS/NIR spectroelectrochemical study was carried out on $[\mathbf{1}]^{n+}$ for n = 3–6; the mixed-valence species $[\mathbf{1}]^{5+}$ displays a narrow π–π* transition at 1534 nm, indicative of a class III mixed-valence state. The chemically generated one-electron-reduced species $[\mathbf{1}]^{3+}$ shows an EPR signal (g = 2.0085) characteristic of a ligand-centred radical. $[\mathbf{1}]^{4+}$ is weakly luminescent at 77 K.

Introduction

There has been considerable research interest in recent years in the study of dinuclear complexes which exhibit a stable mixed-valence state due to a strong electronic interaction across a bridging ligand.[1,2] This interest arises from the relevance of such complexes to biological processes,[3] molecular electronics[4] and for theoretical studies on electron transfer.[5] The degree of electronic communication between the metal centres in the mixed-valence state is primarily controlled by the electronic characteristics of the bridging ligand, which can mediate the electronic interaction through its π-symmetry orbitals by either electron-transfer or hole-transfer mechanisms.[1]

In this context, there has been much recent interest in dinuclear complexes based on a 1,2,4,5-tetrazine bridging unit (abbreviated tz).[6–12] Kaim and co-workers have shown that the tz unit affords exceptionally strong electronic metal–metal interactions in a series of Fe and Ru dinuclear complexes as a consequence of (i) the low-energy LUMO and (ii) the high coefficient of the LUMO on the coordinating N atoms, which allows effective overlap between metal and ligand orbitals.[6–12] Amongst bridging ligands based on the tz unit, the bis-bidentate ligand 3,6-bis-(2-pyridyl)-1,2,4,5-tetrazine (L^1) is the most extensively studied.[8–12] We describe here the synthesis of a new dinuclear complex based on the related, but hitherto unstudied, bridging ligand 3,6-bis-(3,5-dimethylpyrazolyl)-1,2,4,5-tetrazine (L), which was in turn derived from the known[13] compound 3,6-bis-(3,5-dimethylpyrazol-1-yl)-1,4-dihydro-1,2,4,5-tetrazine (H_2L) by spontaneous oxidation during coordination to the metal.

Herein, we report the crystal structure of H_2L, synthesis of the new complex $[(bpy)_2Ru(\mu\text{-}L)Ru(bpy)_2][ClO_4]_4$ (**1**), its crystal structure, electrochemical/spectroscopic properties and its UV/VIS/NIR spectroelectrochemical properties in the four accessible oxidation states.

Results and discussion

H_2L was prepared according to the literature method;[13] its crystal structure is shown in Fig. 1. The bond distances and angles are unremarkable. The most significant feature of the structure is the non-planarity of the central dihydrotetrazine ring, arising from the two formally sp^3-hybridised N atoms.

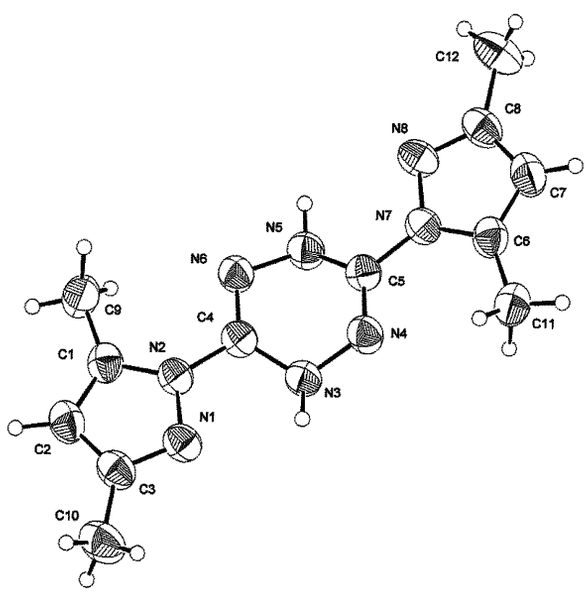

Fig. 1 Crystal structure of H_2L (atoms are drawn at 50% probability).

Although H_2L is stable to oxidation on its own, requiring treatment with strong chemical oxidants to be converted to L,[13] reaction of H_2L with $[Ru(bpy)_2(EtOH)_2]^{2+}$ affords the dinuclear complex $[(bpy)_2Ru(\mu\text{-}L)Ru(bpy)_2]^{4+}$ ($[\mathbf{1}]^{4+}$), in which the bridging

ligand has oxidised to a tetrazine fragment; it was isolated as both its perchlorate and hexafluorophosphate salts. The N–H vibration of H_2L at 3289 cm^{-1} is absent from the IR spectrum of the complex. The ^1H NMR spectrum of [**1**$(ClO_4)_4$] (Fig. 2),

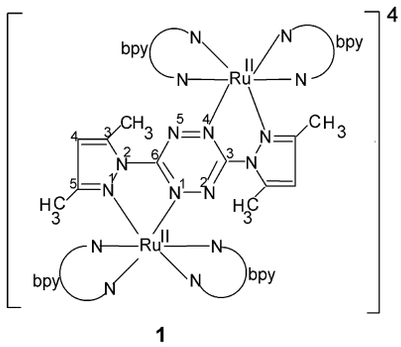

1

in agreement with the expected twofold symmetry of the complex, shows 17 aromatic proton environments: sixteen from the two bipyridyl ligands (overlapping between 7.4 and 9.0 ppm) and one from the pyrazolyl H-4 proton, distinct from the others at 6.52 ppm. That the NH protons of H_2L (*ca.* 8 ppm) are absent in the spectrum of [**1**$(ClO_4)_4$] was confirmed by a D_2O shake, which caused no change in the number or intensity of the signals in this region of the ^1H NMR spectrum. The two methyl signals of the pyrazolyl rings of L, each corresponding to six hydrogen atoms, appear at δ 1.75 and 1.50 ppm. Further confirmation of the formulation of the complex was provided by FAB mass spectrometry, conductivity data and elemental analysis (see Experimental).

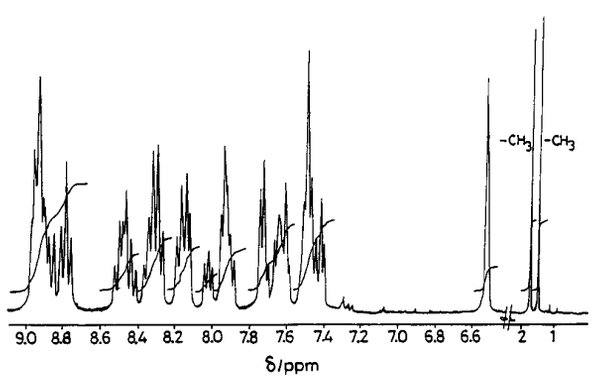

Fig. 2 ^1H NMR spectrum of [**1**$(ClO_4)_4$]·$2H_2O$ in $(CD_3)_2SO$.

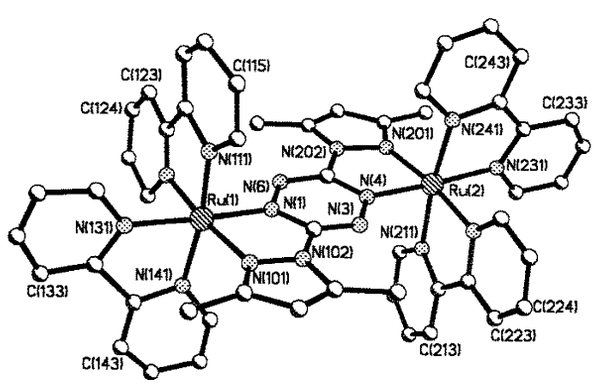

Fig. 3 Crystal structure of [**1**$(ClO_4)_4$]·$2H_2O$ (atoms are drawn at 50% probability).

The crystal structure of [**1**$(ClO_4)_4$]·$2H_2O$ is shown in Fig. 3, and is completely in accord with the spectroscopic data described above. The quality of structural determination is not very high because of problems associated with twinning, but it is clear in particular that the central tetrazine ring is planar and aromatic (in marked contrast to the structure observed for the ligand precursor H_2L described above); the maximum deviation from the mean plane of this ring is 0.036 Å for atom C(5). The coordination geometry about each Ru centre is unremarkable and not worth discussing in detail given the quality of the refinement, except to note that the shortest Ru–N distances are those involving the strongly π-accepting tetrazine unit. Selected bond distances and angles are included in Table 1.

Complex $[\mathbf{1}]^{4+}$ displays two successive reversible one-electron oxidation processes at half-wave potentials $E_{1/2}$ (ΔE_p/mV) of 1.25 (70) (couple I) and 1.70 (100) (couple II) V *versus* SCE (Fig. 4). The one-electron nature of the first couple was

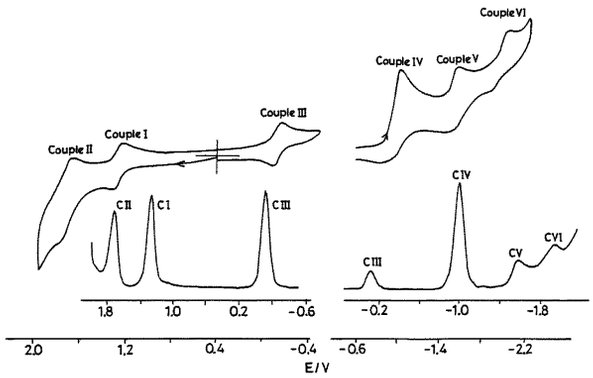

Fig. 4 Cyclic voltammograms and differential pulse voltammograms of $[\mathbf{1}]^{4+}$ in MeCN.

confirmed by constant-potential coulometry. These oxidation processes are assigned as the stepwise oxidations of the two ruthenium(II) centres, *i.e.* two successive Ru(II)/Ru(III) couples separated by 450 mV due to a strong electronic interaction across the tetrazine bridge. The 450 mV separation gives a comproportionation constant (K_c) in the mixed-valence state of *ca.* 4×10^7 [using the equation $RT\ln K_c = nF(\Delta E)$], strongly indicating a class III mixed-valence system.[14] For comparison, the related complex $[(bpy)_2Ru(\mu\text{-}L^1)Ru(bpy)_2]^{4+}$ has a separation of 500 mV between the successive Ru(II)/Ru(III) couples,[11] corresponding to $K_c \approx 3 \times 10^8$; replacement of the pyridyl units in the bridging ligand L^1 by pyrazolyl units in L has resulted in a modest diminution of the metal–metal electronic interaction. Comparison of the absolute values of the redox potentials in the two complexes indicates that the π-acceptor strength of L is less than that of L^1 as the metal-centred redox potentials are less positive.[11]

Complex $[\mathbf{1}]^{4+}$ also displays four successive reduction processes at half-wave potentials $E_{1/2}$ (ΔE_p/mV) of −0.13 (70) (couple III), −0.99 (130) (couple IV), −1.58 (100) (couple V) and −1.94 (120) (couple VI) V *versus* SCE (Fig. 4). The one-electron nature of couple III (which is reversible) was confirmed by a constant potential coulometric experiment; reduction at more negative potentials results in decomposition as couple IV is irreversible. While the potentials of couples V and VI are in the region consistent with them being bpy-based reduction {*cf.* the reductions of $[Ru(bpy)_3]^{2+}$, which occur between −1.3 and −1.8 V *versus* SCE},[15] the modest potentials of couples III and IV indicate that they involve the LUMO of the bridging ligand L, which is dominated by the central π-acidic tetrazine moiety.[6–12] This behaviour may be contrasted with that of free H_2L in acetonitrile, which displays only irreversible processes at −0.9 and +0.49 V *versus* SCE, the latter being the $2e^-/2H^+$ process which generates the aromatic tetrazine ring of L.[13]

In acetonitrile, [**1**][PF_6]$_4$ exhibits four strong transitions [λ_{max}/nm (ε/dm^3 mol^{-1} cm^{-1}): 757 (15 000); 400 (7000); 283 (50 000); 246 (24 000)] (Fig. 5). The strong transitions in the UV region are ligand-centred $\pi \longrightarrow \pi^*$ processes, and the two lower-energy transitions at 757 and 400 nm are assigned as Ru(II) $\longrightarrow \pi^*$ (L) and Ru(II) $\longrightarrow \pi^*$ (bpy) MLCT transitions, respectively.[11,15] This

Table 1 Selected bond lengths (Å) and angles (°) for $[\mathbf{1}(ClO_4)_4]\cdot 2H_2O$

Ru(1)–N(1)	1.976(14)	Ru(2)–N(201)	2.000(14)
Ru(1)–N(111)	1.995(15)	Ru(2)–N(241)	2.031(16)
Ru(1)–N(121)	2.012(17)	Ru(2)–N(211)	2.070(18)
Ru(1)–N(141)	2.02(2)	Ru(2)–N(231)	2.072(14)
Ru(1)–N(131)	2.08(2)	Ru(2)–N(221)	2.093(18)
Ru(1)–N(101)	2.114(16)	N(1)–N(6)	1.34(2)
Ru(2)–N(4)	1.993(11)	N(3)–N(4)	1.369(19)
N(1)–Ru(1)–N(111)	90.3(7)	N(4)–Ru(2)–N(201)	78.3(6)
N(1)–Ru(1)–N(121)	95.7(6)	N(4)–Ru(2)–N(211)	87.4(6)
N(1)–Ru(1)–N(141)	99.6(7)	N(4)–Ru(2)–N(221)	92.7(6)
N(1)–Ru(1)–N(131)	177.3(7)	N(4)–Ru(2)–N(231)	177.0(6)
N(1)–Ru(1)–N(101)	78.0(7)	N(4)–Ru(2)–N(241)	98.4(7)
N(111)–Ru(1)–N(121)	85.0(8)	N(201)–Ru(2)–N(211)	96.1(7)
N(111)–Ru(1)–N(141)	170.0(7)	N(201)–Ru(2)–N(221)	170.8(6)
N(111)–Ru(1)–N(131)	87.1(7)	N(201)–Ru(2)–N(231)	99.8(6)
N(111)–Ru(1)–N(101)	92.2(6)	N(201)–Ru(2)–N(241)	88.4(7)
N(121)–Ru(1)–N(141)	94.0(8)	N(211)–Ru(2)–N(221)	81.3(8)
N(121)–Ru(1)–N(131)	83.4(7)	N(211)–Ru(2)–N(231)	95.1(8)
N(121)–Ru(1)–N(101)	173.1(7)	N(211)–Ru(2)–N(241)	173.2(7)
N(131)–Ru(1)–N(141)	83.0(7)	N(221)–Ru(2)–N(231)	89.3(6)
N(131)–Ru(1)–N(101)	102.8(7)	N(221)–Ru(2)–N(241)	95.0(7)
N(141)–Ru(1)–N(101)	89.9(7)	N(231)–Ru(2)–N(241)	79.1(8)

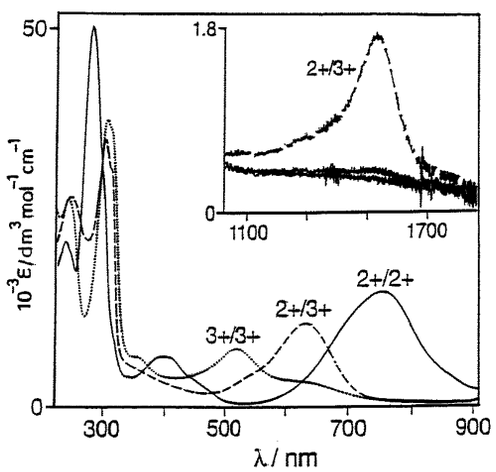

Fig. 5 UV/VIS/NIR spectra of $[\mathbf{1}]^{4+}$ (solid line), $[\mathbf{1}]^{5+}$ (dashed line) and $[\mathbf{1}]^{6+}$ (dotted line) in MeCN at 243 K. The metal oxidation state combinations are indicated in each curve.

is in agreement with the observation that the bridging ligand L reduces more easily than do the bpy ligands, in agreement with many other reports[8–12] and with our assignment of the electrochemical data; this finds further justification from the spectroelectrochemical correlation data. The energies of the MLCT transitions can be predicted with the help of eqn. 1 and 2:[16]

$$\nu(\text{MLCT}) = 8065\ (\Delta E_{1/2}) + 3000 \quad (1)$$

$$\Delta E_{1/2} = E_{1/2}(\text{Ru}^{\text{III}} - \text{Ru}^{\text{II}}) - E_{1/2}(\text{ligand}) \quad (2)$$

where $E_{1/2}(\text{Ru}^{\text{III}} - \text{Ru}^{\text{II}})$ is the formal potential (in V) of the reversible first Ru(III)/Ru(II) couple (couple I), $E_{1/2}$(ligand) is the first ligand-based reduction (either L or bpy-based, as appropriate) and ν (MLCT) is the predicted wavenumber of the charge-transfer band in cm^{-1}. From these equations, and the values of + 1.25 V for $E_{1/2}(\text{Ru}^{\text{III}} - \text{Ru}^{\text{II}})$, −0.13 V for $E_{1/2}$(L) and −1.58 V for $E_{1/2}$(bpy), the calculated MLCT energies are 14129 and 25824 cm^{-1}, which agree reasonably well with the observed ν (MLCT) energies, 13210 and 25000 cm^{-1}, respectively.

Electrochemical oxidation of $[\mathbf{1}]^{4+}$ (as its hexafluorophosphate salt) in CH_3CN at 243 K using a thermostatted OTTLE cell initially generates the mixed-valence Ru(II)/Ru(III) species $[\mathbf{1}]^{5+}$. The Ru(II)-based MLCT transition of $[\mathbf{1}]^{4+}$ is reduced in intensity and blue shifted to 633 nm (Fig. 5). In addition, a narrow π–π* band appears at 1534 nm (ε, 1800 $dm^3\ mol^{-1}\ cm^{-1}$), with a width at half height ($\Delta\nu_{1/2}$) of 650 cm^{-1}. The narrowness of this transition is indicative of class III behaviour. For a class II complex, the relationship

$$\Delta\nu_{1/2} = (2310E_{\text{op}})^{1/2} \quad (3)$$

(derived from Hush theory) is expected to hold, which would give a value for $\Delta\nu_{1/2}$ of nearly 3900 cm^{-1} (E_{op} is the energy of the π–π* band maximum in cm^{-1}).[1e,g] In contrast, for class III complexes, the value of $\Delta\nu_{1/2}$ is expected to be much less than this, as is the case here; assignment of class III character is also indicated by the 450 mV separation between the Ru(II)/Ru(III) couples. In this case, the value of the electronic coupling parameter V_{ab} is just $E_{\text{op}}/2$, *i.e.* 3260 cm^{-1} in this complex.[1e,g] Although the electronic spectrum of the analogous mixed-valence complex[11] $[(bpy)_2Ru(\mu\text{-}L^1)Ru(bpy)_2]^{4+}$ has not been reported, many related Fe(II)/Fe(III) and Ru(II)/Ru(III) complexes with tz-based bridging ligands have been assigned as having class III mixed-valence states.[6–12]

On further oxidation to $[\mathbf{1}]^{6+}$, the remaining Ru(II)-based MLCT transitions and the π–π* transition disappear and are replaced by a moderately intense transition at 522 nm (Fig. 5), which we assign as a ligand ⟶ Ru(III) LMCT transition involving either the bridging ligand L or the terminal bpy ligands.[17] It is noticeable how the lowest energy charge-transfer transition of the mixed-valence complex $[\mathbf{1}]^{5+}$ is mid-way in position and intensity between those of $[\mathbf{1}]^{4+}$ and $[\mathbf{1}]^{6+}$: *i.e.* a single 'averaged' transition is seen rather than two distinct transitions characteristic of localised Ru(II) and Ru(III) termini. This provides additional evidence for assignment of the mixed-valence state as class III.

The electrochemically generated one-electron reduced species $[\mathbf{1}]^{3+}$ exhibits two strong bands in the visible region at 622 and 445 nm (Fig. 6). Thus, on moving from $[\mathbf{1}]^{4+} \longrightarrow [\mathbf{1}]^{3+}$, the Ru(II) ⟶ L band is found to be blue shifted from 757 to 622 nm with a drop in intensity, exactly the expected consequence of putting an electron into the acceptor orbital (LUMO of L).[8] The Ru(II) ⟶ bpy MLCT transition, in contrast, is red shifted from 400 to 445 nm with an increase in intensity. This is again consistent with tz-based reduction, as the tz-based radical anion will help to stabilise the +3 charge on the metal centre that arises following the Ru(II) ⟶ bpy MLCT transition. There are no strong transitions in the visible region arising from the tz radical anion.[8] The ligand-radical form $[\mathbf{1}]^{3+}$ was also generated chemically by reduction of a solution in MeCN with hydrazine hydrate; this species shows a sharp EPR signal in fluid solution at g = 2.0085 with a peak–peak separation of 45 G; there is some poorly-resolved fine structure which we assume to be hyperfine coupling to the N atoms (Fig. 7). This g value, and the

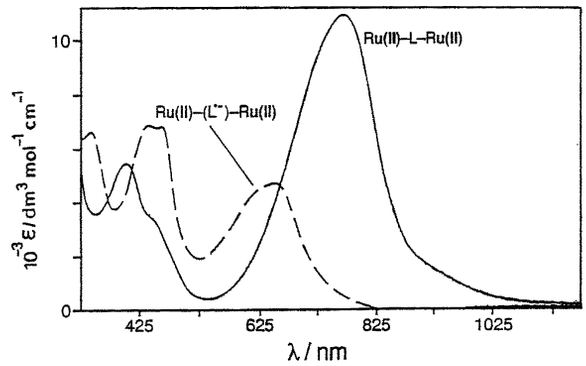

Fig. 6 UV-visible spectra of $[\mathbf{1}]^{4+}$ (solid line) and $[\mathbf{1}]^{3+}$ (dashed line) in MeCN at 243 K.

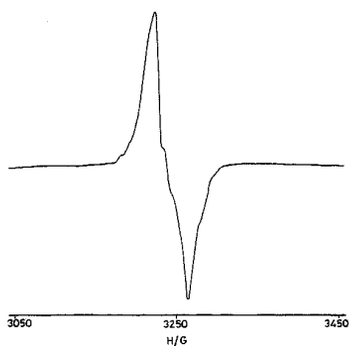

Fig. 7 X-Band EPR spectrum of chemically reduced complex $[\mathbf{1}]^{3+}$ in MeCN at 77 K.

clear presence of hyperfine coupling to the N atoms, are both indicative of a largely tz-centred radical.[18]

The influence of pH on the absorption spectrum of $[\mathbf{1}]^{4+}$ has been examined in acetonitrile–water (2 : 1). In the (apparent) pH range 2.7 to 0.1, the lowest energy Ru(II) ⟶ L MLCT band is red shifted from 660 to 756 nm (Fig. 8). This process, which is

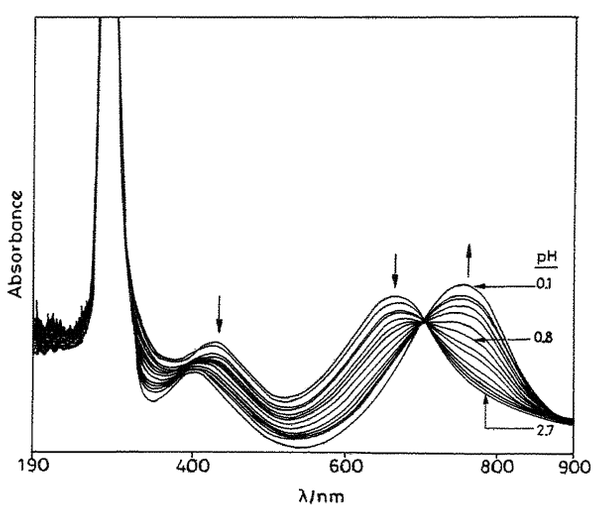

Fig. 8 Changes in the UV-visible spectrum of $[\mathbf{1}]^{4+}$ as the pH is varied (pH = 2.7–0.1) in MeCN–H_2O (2 : 1).

reversible, has a pK_a value of 1.0 and may be assigned to protonation of one of the non-coordinated N atoms of the central tetrazine fragment, which will have the effect of reducing the LUMO in energy and stabilising the Ru(II) ⟶ L MLCT transition, as observed. For comparison, the pK_a value of pyrazine is reported to be 0.6.[19] Under very basic conditions (pH ≈ 12), the solution becomes dark and irreversible decomposition occurs.

Finally, we note that the complex is weakly luminescent. In a methanol–ethanol glass (1 : 4) at 77 K, the two lowest energy MLCT transitions are at 451 [Ru(II) ⟶ π*(bpy) MLCT] and

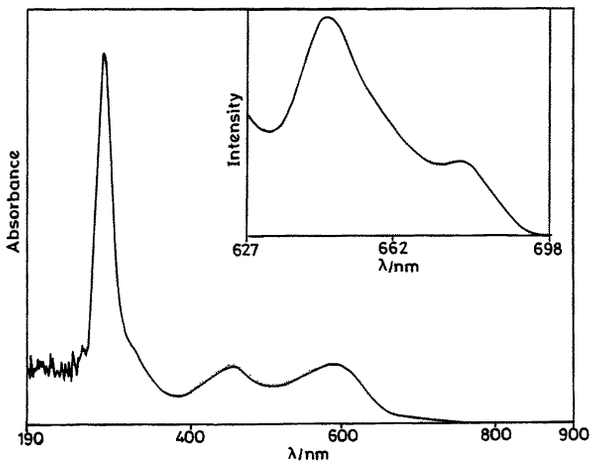

Fig. 9 UV-visible spectrum of $[\mathbf{1}]^{4+}$ in MeOH–EtOH (1 : 4). The inset shows the emission spectrum in methanol–ethanol (1 : 4) glass at 77 K.

595 nm [Ru(II) ⟶ π*(L) MLCT] (Fig. 9). Excitation at 451 nm results in weak emission at 647 nm (quantum yield $\Phi = 8 \times 10^{-3}$), with vibrational fine structure characteristic of emission from a ^{3}MLCT excited state, presumably involving the bridging ligand L.[15]

Experimental

General details

The starting materials *cis*-$[Ru(bpy)_2Cl_2]\cdot 2H_2O$ and H_2L were prepared according to the reported procedures.[20,13] The instruments used for the standard spectroscopic and electrochemical experiments have been described elsewhere.[21,22] The spectroelectrochemistry studies were performed at 243 K in an OTTLE cell mounted in the sample compartment of a Perkin Elmer Lambda 19 spectrophotometer, as described previously.[22] Fluorescence quantum yields were determined using a previously described method.[23]

Preparation of 1

A mixture of $[Ru(bpy)_2Cl_2]\cdot 2H_2O$ (0.265 g, 0.5 mmol) and $AgClO_4$ (0.220g, 1.0 mmol) in ethanol was heated with constant stirring for 1.5 h. The resultant AgCl precipitate was filtered off after cooling to give a red solution of $[Ru(bpy)_2(EtOH)_2]^{2+}$. To this was added H_2L (0.070 g, 0.25 mmol) and the mixture was refluxed under a dinitrogen atmosphere overnight, whereupon a green solid compound precipitated. The reaction mixture was cooled and filtered. The green solid, $[(bpy)_2Ru(\mu\text{-}L)Ru(bpy)_2](ClO_4)_4\cdot 2H_2O$, thus obtained was washed thoroughly with ethanol and then recrystallised from dichloromethane–hexane (1 : 3). Yield 0.234 g (60%). Anal. calcd. for $\mathbf{1}(ClO_4)_4\cdot 2H_2O$: C, 40.7; H, 3.4; N, 14.6; found: C, 41.7; H, 3.3; N, 15.0%. Conductivity: Λ_M ($cm^2\ \Omega^{-1}\ mol^{-1}$): 419.

A small quantity of $\mathbf{1}(ClO_4)_4$ was converted to the hexafluorophosphate salt $\mathbf{1}(PF_6)_4$ for electrochemical and spectroelectrochemical studies. Excess aqueous KPF_6 was added to the perchlorate salt $[\mathbf{1}(ClO_4)_4]$ in MeCN until the complex precipitated, and recrystallised from MeCN–diethyl ether. FAB-MS: *m/z* 1388 [100%, $\{\mathbf{1}(PF_6)_2\}^{2+}$]. The ^{1}H NMR spectrum of complex $\mathbf{1}(PF_6)_4$ in $(CD_3)_2SO$ was found to be identical to that of the perchlorate derivative.

Crystallography

Cube-like single crystals of H_2L were grown by slow diffusion of a dichloromethane solution in hexane, followed by slow evaporation. X-Ray data for H_2L were collected on a PC-controlled Enraf-Nonius CAD-4 (MACH-3) single crystal X-ray diffractometer using Mo-Kα radiation. Significant crystallographic parameters are listed in Table 2. The structure

Table 2 Crystallographic data for H_2L and $[\mathbf{1}(ClO_4)_4]\cdot 2H_2O$

Compound	H_2L	$[\mathbf{1}(ClO_4)_4]\cdot 2H_2O$
Empirical formula	$C_{12}H_{16}N_8$	$C_{52}H_{50}Cl_4N_{16}O_{18}Ru_2$
FW	272.33	1531.02
Crystal system	Monoclinic	Orthorhombic
Space group	$P2_1/c$	$Pca2_1$
a/Å	11.1301(8)	23.861(3)
b/Å	11.0060(9)	13.452(2)
c/Å	11.4837(10)	19.238(3)
β/°	100.492(7)	90
V/Å^3	1383.21(19)	6175.0(16)
Z	4	4
Instrument used	Nonius MACH3	Bruker SMART-CCD
T/K	293(2)	173(2)
ρ_{calcd}/g cm^{-3}	1.308	1.647
Abs. coeff./mm^{-1}	0.088	0.0746
Data/restraints/parameters	2434/0/186	5758/61/557
Final R_1, wR_2	0.0514, 0.1528	0.0790, 0.1977

was solved by direct methods using SHELXS-86 and refined by full-matrix least squares on F^2 using SHELXL-97.[24]

Crystals of $[\mathbf{1}(ClO_4)_4]\cdot 2H_2O$ were grown by slow diffusion of an acetonitrile solution of $[\mathbf{1}(ClO_4)_4]\cdot 2H_2O$ into benzene, followed by slow evaporation. Crystal data and the data collection parameters are given in Table 2. A crystal of approximate dimensions 0.2 × 0.2 × 0.1 mm was mounted on a Siemens SMART diffractometer in a cold N_2 stream at 173 K. The structure was solved and refined by full-matrix least squares on F^2 using the SHELX suite of programs,[25] the data set was absorption-corrected using SADABS.[26]

Structure solution and refinement were complicated by the fact that the crystals, which have the chiral space group $Pca2_1$, diffracted very weakly due to enantiomeric twinning. Consequently, only data with $2\theta \leq 40°$ were used in the final refinement as there was no significant diffracted intensity at higher angles. Only the Ru, N and Cl atoms, and the O atoms of three of the perchlorate anions, were refined with anisotropic thermal parameters. Attempts to refine more of the atoms anisotropically resulted in the refinement becoming unstable. One of the perchlorate anions was disordered over two sites with equal site occupancies; the O atom of this anion was refined isotropically. Apart from the complex cation and the four anions, two significant residual electron density peaks which were located *ca.* 3 Å from perchlorate O atoms (*i.e.* typical O–H ··· O hydrogen-bonding distance) were refined as O atoms of water molecules. The overall quality of the refinement is not particularly high (R_1 = 0.079), but the important features of the structure are clear.

CCDC reference numbers 170798 and 178079.

See http://www.rsc.org/suppdata/dt/b1/b108296e/ for crystallographic data in CIF or other electronic format.

Acknowledgements

Financial support received from the Council of Scientific and Industrial Research, New Delhi (India), and the University of Bristol (UK) is gratefully acknowledged. Special acknowledgment is made to Regional Sophisticated Instrumentation Center, RSIC, Indian Institute of Technology, Bombay, for providing NMR and EPR facilities. The X-ray structural studies of H_2L were carried out at the National Single Crystal Diffractometer Facility, Indian Institute of Technology, Bombay. M. D. W. is the Royal Society of Chemistry Sir Edward Frankland Fellow for 2000–2001.

References

1 Reviews: (*a*) W. Kaim, A. Klein and M. Glöckle, *Acc. Chem. Res.*, 2000, **33**, 755; (*b*) J. A. McCleverty and M. D. Ward, *Acc. Chem. Res.*, 1998, **31**, 842; (*c*) D. Astruc, *Acc. Chem. Res.*, 1997, **30**, 383; (*d*) M. D. Ward, *Chem. Soc. Rev.*, 1995, **24**, 121; (*e*) R. J. Crutchley, *Adv. Inorg. Chem.*, 1994, **41**, 273; (*f*) G. Giuffrida and S. Campagna, *Coord. Chem. Rev.*, 1994, **135–136**, 517; (*g*) C. Creutz, *Prog. Inorg. Chem.*, 1983, **30**, 1.

2 Recent examples: (*a*) P. J. Mosher, G. P. A. Yap and R. J. Crutchley, *Inorg. Chem.*, 2001, **40**, 1189; (*b*) R. H. Laye, S. M. Couchman and M. D. Ward, *Inorg. Chem.*, 2001, **40**, 4089; (*c*) W. E. Meyer, A. J. Amoroso, C. R. Horn, M. Jaeger and J. A. Gladysz, *Organometallics*, 2001, **20**, 1115; (*d*) J. E. Ritchie and R. W. Murray, *J. Am. Chem. Soc.*, 2000, **122**, 2964; (*e*) T. Weyland, K. Coustas, L. Toupet, J. F. Halet and C. Lapinte, *Organometallics*, 2000, **19**, 4228; (*f*) J.-P. Launay, S. Fraysse and C. Coudret, *Mol. Cryst. Liq. Cryst.*, 2000, **344**, 125; (*g*) S. Baitalik, U. Florke and K. Nag, *J. Chem. Soc., Dalton Trans.*, 1999, 719.

3 E. I. Solomon, T. C. Brunold, M. I. Davis, J. N. Kemsley, S. K. Lee, N. Lehnert, F. Neese, A. J. Skulan, Y. S. Yang and J. Zhou, *Chem. Rev.*, 2000, **100**, 235.

4 (*a*) F. Paul and C. Lapinte, *Coord. Chem. Rev.*, 1998, **178–180**, 431; (*b*) M. D. Ward, *Chem. Ind.*, 1996, 568; (*c*) M. D. Ward, *Chem. Ind.*, 1997, 640.

5 (*a*) B. S. Brunschwig and N. Sutin, *Coord. Chem. Rev.*, 1999, **187**, 233; (*b*) A. Bencini, I. Ciofini, C. A. Daul and A. Ferretti, *J. Am. Chem. Soc.*, 1999, **121**, 11418.

6 M. Glockle, W. Kaim, A. Klein, E. Roduner, G. Hubmer, S. Zalis, J. Slageren, F. Renz and P. Gutlich, *Inorg. Chem.*, 2001, **40**, 2256.

7 M. Glockle, K. Hubler, H.-J. Kummerer, G. Denninger and W. Kaim, *Inorg. Chem.*, 2001, **40**, 2263.

8 T. Scheiring, J. Fiedler and W. Kaim, *Organometallics*, 2001, **20**, 1437.

9 G. Markus, W. Kaim, N. E. Katz, M. G. Posse and E. H. Cutin, *Inorg. Chem.*, 1999, **38**, 3270.

10 J. Poppe, M. Moscherosch and W. Kaim, *Inorg. Chem.*, 1993, **32**, 2640.

11 W. Kaim and V. Kasack, *Inorg. Chem.*, 1990, **29**, 4696.

12 S. Ernst, V. Kasack and W. Kaim, *Inorg. Chem.*, 1988, **27**, 1146.

13 M. D. Coburn, G. A. Buntain, B. W. Harris, M. A. Hiskey, K. Y. Lee and D. G. Ott, *J. Heterocycl. Chem.*, 1991, **28**, 2049.

14 M. B. Robin and P. Day, *Adv. Inorg. Chem. Radiochem.*, 1967, **10**, 247.

15 A. Juris, V. Balzani, F. Barigelletti, S. Campagna, P. Belser and A. Von Zelewsky, *Coord. Chem. Rev.*, 1988, **84**, 85.

16 (*a*) B. K. Ghosh and A. Chakravorty, *Coord. Chem. Rev.*, 1989, **95**, 239; (*b*) B. K. Santra and G. K. Lahiri, *J. Chem. Soc., Dalton Trans.*, 1997, 129; (*c*) E. S. Dosworth and A. B. P. Lever, *Chem. Phys. Lett.*, 1986, **124**, 152.

17 (*a*) G. M. Bryant and J. E. Ferguson, *Aust. J. Chem.*, 1971, **24**, 275; (*b*) R. J. P. Williams, *J. Am. Chem. Soc.*, 1953, **75**, 2163.

18 (*a*) W. Kaim and S. Kohlmann, *Inorg. Chem.*, 1986, **25**, 3442; (*b*) W. Kaim, S. Ernst, S. Kohlmann and P. Welkerling, *Chem. Phys. Lett.*, 1985, **118**, 431.

19 J. A. Dean, *Lange's Handbook of Chemistry*, McGraw Hill, New York, 13th edn., 1985.

20 B. P. Sullivan, D. J. Salmon and T. J. Meyer, *Inorg. Chem.*, 1978, **17**, 3334.

21 R. Samanta, B. Mondal, P. Munshi and G. K. Lahiri, *J. Chem. Soc., Dalton Trans.*, 2001, 1827.

22 S.-M. Lee, R. Kowallick, M. Marcaccio, J. A. McCleverty and M. D. Ward, *J. Chem. Soc., Dalton Trans.*, 1998, 3443.

23 (*a*) R. Alsfasser and R. van Eldik, *Inorg. Chem.*, 1996, **35**, 628; (*b*) P. Chen, R. Duesing, D. K. Graff and T. J. Meyer, *J. Phys. Chem.*, 1991, **95**, 5850.

24 G. M. Sheldrick, SHELXS-97, Program for Crystal Structure Solution and Refinement, University of Göttingen, Germany, 1997.

25 SHELXTL program system, version 5.1, Bruker Analytical X-Ray Instruments Inc., Madison, WI, 1998.

26 G. M. Sheldrick, SADABS, Program for Absorption Correction with the Siemens SMART Area-Detector System, University of Göttingen, Germany, 1996.